INTERNATIONAL JOURNAL FOR NUMERICAL METHODS IN FLUIDS
Int. J. Numer. Meth. Fluids 2005; **48**:99–106
Published online 25 February 2005 in Wiley InterScience (www.interscience.wiley.com). DOI: 10.1002/fld.945

Computation of the flow in a ventilated room using non-linear RANS, LES and hybrid RANS/LES‡

Alexandre Jouvray*,† and Paul G. Tucker

Civil and Computational Engineering Centre, School of Engineering, University of Wales, Swansea SA2 8PP, U.K.

SUMMARY

The isothermal flow in an empty ventilated room is computed. Performances of linear and non-linear RANS, LES and a hybrid RANS/LES (LNS) models are compared. When compared to linear equivalents, the non-linear RANS models are found to modestly improve predicted velocities and Reynolds stresses. Generally, best agreement is found between measurements and LES. Also, the LNS appears a promising model, giving the best velocity agreement and overall good agreement with measured Reynolds stresses. However, the method has the potential for LES zones to occur downstream of RANS zones. This gives rise to poor LES boundary conditions. Hence the current LNS results could be fortuitous. Copyright © 2005 John Wiley & Sons, Ltd.

KEY WORDS: turbulence; non-linear eddy–viscosity RANS; hybrid RANS/LES; LNS; room-ventilation

1. INTRODUCTION

The modelling of flows in rooms has become a topic of great importance in the last decade. This is because studies have revealed the association between health and indoor air quality [1]. Also there has been an increase in building health and safety regulations [2]. Room ventilation predictions are generally made for complex geometries using relatively simple turbulence models (i.e. Reference [3]). The simple, empty room geometry studied here (see Figure 1(a)) does not present any significant problem-definition issues. Hence, a wide range of turbulence models have been tested without the assessment of solution accuracies being clouded by problem definition uncertainties. The turbulence models tested are as follows: Mixing lengths (*ml*1 and *ml*2), k–l [4], k–ε [3], EASM [5] (in either a k–l or k–ε framework),

*Correspondence to: Alexandre Jouvray, Civil and Computational Engineering Centre, School of Engineering, University of Wales, Swansea SA2 8PP, U.K.
†E-mail: alex_jouvray@hotmail.com
‡This was originally submitted as part of the ICFD SPECIAL ISSUE.

Received 27 April 2004
Revised 21 May 2004
Accepted 31 January 2005

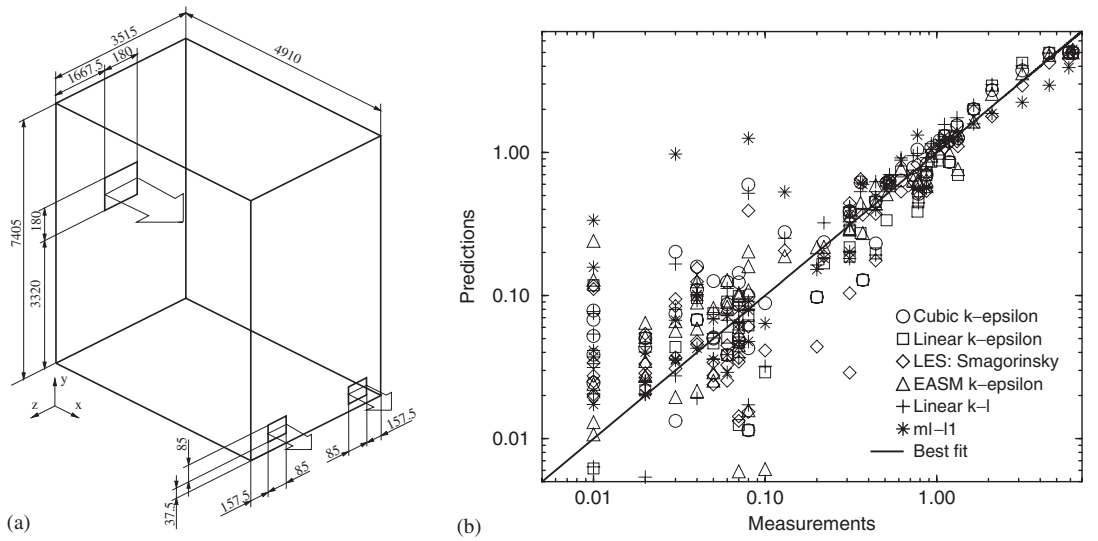

Figure 1. (a) Definition of the empty ventilated room; and (b) comparison of predicted velocities with measurements (%).

cubic [6] (k–ε), LES-1 [7], LES-2 [8], and LNS [9]. A brief description of the more advanced models used in this work is given in Section 2. The predictions here are compared against measurements recorded over 144 points in the empty ventilated room of Reference [10].

2. TURBULENCE MODELLING AND NUMERICAL METHODS

The RANS, LES and hybrid RANS/LES models used in this study are briefly described below. The RANS models are the *ml*1, *ml*2, k–ε, k–l, EASM and cubic. For the mixing length models *ml*1 and *ml*2, in the inlet jet region the mixing length is altered using established corrections. For *ml*1, the mixing length (l_m) is taken as $0.075L$ and for *ml*2, $l_m = 0.09L$ where L is the jet half-width. The well documented and validated low Reynolds number version of the k–ε [11] is used in this study. With the adverse pressure gradients in the current flow this choice seems reasonable. The low Reynolds number k–l model uses the damping function as defined by Wolfshtein [4]. The EASM [5] and cubic eddy–viscosity [6] models have been developed to describe the flow in a more physically consistent manner. The EASM is a computationally inexpensive alternative to the Algebraic Stress Model. Using the EASM, the Reynolds stress tensor is defined as

$$\tau_{ij} = -\frac{2}{3}\rho k\delta_{ij} + 2\mu_{t_1}S_{ij} + 2\mu_{t_2}\frac{k}{\varepsilon}(S_{ik}W_{kj} + S_{jk}W_{ki}) - 4\mu_{t_3}\frac{k}{\varepsilon}\left(S_{ik}S_{kj} - \frac{1}{3}S_{mn}S_{mn}\delta_{ij}\right) \quad (1)$$

where S_{ij} and W_{ij} are the strain and vorticity rate. The turbulent viscosity μ_{t_i} is evaluated as $\mu_{t_i} = \rho C_{\mu_i} k^2/\varepsilon$. Recent trends in turbulence modelling seem to account for the fact that C_μ ($= 0.09$ for the linear k–ε model) is not a constant and depends on the flow itself. Here it is

defined in a tensor form as

$$C_{\mu 1} = \alpha_1 \left[\frac{3(1+\eta^2)}{3+\eta^2+6\zeta^2\eta^2+6\zeta^2} \right], \quad C_{\mu 2,3} = \alpha_1 \alpha_{2,3} \left[\frac{3(1+\eta^2)}{3+\eta^2+6\zeta^2\eta^2+6\zeta^2} \right] \tag{2}$$

where η and ζ are known as the invariance coefficients defined as

$$\eta = \frac{1}{2} \frac{\alpha_3}{\alpha_1} \frac{k}{\varepsilon} (S_{ij} S_{ij})^{1/2}, \quad \zeta = \frac{\alpha_2}{\alpha_1} \frac{k}{\varepsilon} (W_{ij} W_{ij})^{1/2} \tag{3}$$

The coefficients α_i and g are

$$\alpha_1 = 0.5 \left(\frac{4}{3} - C_1 \right) g, \quad \alpha_2 = 0.5(2 - C_2) g, \quad \alpha_3 = 0.5(2 - C_3) g, \quad g = \left(0.5\, C_4 + \frac{P_k}{\varepsilon} - 1 \right)^{-1} \tag{4}$$

The following constants are used: $C_1 = 0.36$, $C_2 = 0.4$, $C_3 = 1.25$ and $C_4 = 6.8$.

The cubic eddy–viscosity model [6] is also tested. The use of cubic terms has the distinct advantage over linear and quadratic terms of capturing streamline curvature. The Reynolds stress is calculated by Equation (5).

$$\begin{aligned} \tau_{ij} = & -\frac{2}{3} \rho \delta_{ij} + 2\mu_t S_{ij} - 4C_1 \frac{\mu_t k}{\tilde{\varepsilon}} \left(S_{ij} S_{kj} - \frac{1}{3} S_{mn} S_{mn} \delta_{ij} \right) - 4C_2 \frac{\mu_t k}{\tilde{\varepsilon}} (W_{ik} S_{kj} + W_{jk} S_{ki}) \\ & - 4C_3 \frac{\mu_t k}{\tilde{\varepsilon}} \left(W_{ik} W_{jk} - \frac{1}{3} W_{mn} W_{mn} \delta_{ij} \right) - 8C_4 \frac{\mu_t k^2}{\tilde{\varepsilon}^2} (S_{ki} W_{lj} + S_{kj} W_{li}) S_{kl} \\ & - 8C_5 \frac{\mu_t k^2}{\tilde{\varepsilon}^2} \left(W_{il} W_{lm} S_{mj} + S_{il} W_{lm} W_{mj} - \frac{2}{3} [S_{lm} W_{mn} W_{nl} \delta_{ij}] \right) \\ & - 8C_6 \frac{\mu_t k^2}{\tilde{\varepsilon}^2} (S_{ij} S_{mn} S_{mn}) - 8C_7 \frac{\mu_t k^2}{\tilde{\varepsilon}^2} (W_{ij} W_{mn} W_{mn}) \end{aligned} \tag{5}$$

The coefficients C_i have been defined using empirical calibrations based on various shear flow configurations. They are defined as: $C_1 = -0.1$, $C_2 = 0.1$, $C_3 = 0.26$, $C_4 = -1.0$, $C_5 = 0.0$, $C_6 = -0.1$ and $C_7 = 0.1$. The turbulent viscosity μ_t is evaluated using the standard k–ε model ($\mu_t = \rho C_\mu f_\mu k^2/\varepsilon$) expression. Here again, C_μ is introduced as the following flow-dependent variable:

$$C_\mu = \frac{0.3}{1.0 + 0.35[\mathrm{Max}(S^*; W^*)]^{3/2}} \left[1.0 - e \left[\frac{-0.36}{e(-0.75\, \mathrm{Max}(S^*; W^*))} \right] \right] \tag{6}$$

where S^* and W^* are the dimensionless strain and vorticity rate.

In LES a separation of eddy scales is assumed. The larger are resolved whereas the smaller eddies (universal in nature) are modelled by a sub-grid stress. To approximately resolve the periodic bursts, ejections and streaks in a turbulent boundary layer using LES, grid requirements are in the order of $\Delta x^+ \simeq 100$, $\Delta y^+ \simeq 1$ and $\Delta z^+ \simeq 20$ [12]. This high grid requirement combined with unsteady modelling makes LES computationally expensive. The large physical dimensions and geometrical complexity of rooms makes LES simulations challenging.

However, fortunately the relatively low Reynolds numbers ease grid demands. In this work, the LES-1 [7] and LES-2 [8] models are used.

The hybrid RANS/LES models have been developed as a compromise between the high accuracy of the LES and the low computational expense of RANS models. Hybrid RANS/LES are found under two main categories: Zonal models (see References [13, 14]) and embedded models. The LNS [9] model is an embedded hybrid RANS/LES model in which no fixed boundary exists between the RANS and the LES part of the flow. The transition between RANS and LES is achieved by scaling the effect of the turbulent viscosity of the RANS model (see Reference [15]). The scaling coefficient used (α) is defined as a function of a turbulent length and velocity scale for both the RANS and the LES models. In this study, the LNS model makes use of the cubic (k–ε) and the LES-1 [7] model. Using these base models α is defined as follows:

$$\alpha = \frac{\mathrm{Min}\left(C_s(\Delta^2 S_{ij}^*, C_\mu k^2/\varepsilon + \Omega)\right)}{C_\mu k^2/\varepsilon + \Omega} \tag{7}$$

where C_s is the Smagorinsky constant (0.05), Δ the grid spacing (taken as $\mathrm{Max}(\delta_x, \delta_y, \delta_z)$) and Ω is a small number used to avoid a singularity.

The turbulence models have been implemented in the NEAT solver [16] and validated for a selection of benchmark problems (see Reference [17]) including plane and sharply turned channel flows, the flow over a backwards facing step and secondary motions (Prandtl's motions of the second kind) in a square duct.

NEAT is a finite volume solver that uses a structured staggered grid arrangement [18]. The results presented here use the second-order central difference scheme for both the convection and diffusion terms. For LES and hybrid simulations the Crank–Nicolson time scheme is used. The inlet flow is assumed uniform, unidirectional and the flow isothermal. A modest grid of $49 \times 71 \times 85$ nodes is used giving a first off wall average $y^+ \simeq 0.7$ with $\delta z^+ \simeq 17$.

3. RESULTS AND DISCUSSION

3.1. Velocity at the jet centreline

Figure 1(b) plots predicted against measured velocities for the 144 measurement points for a range of models. If all the models worked perfectly the points would all collapse on the 45° line. The figure shows that, overall, solution accuracy increases with velocity. This may partly be explained by measurement inaccuracy at lower velocities. The overall flow in the room is governed by the jet-like inlet. Figure 2(a) compares velocity profiles along the centreline of the inlet jet for a selection of models.

It shows that non-linear eddy viscosity models (EVM) improve velocity predictions compared with linear EVM. The improvements are however not of significant magnitude ($< 10\%$). Overall, the cubic model predictions are more accurate than the EASM. The LES-1 [7] and LNS [9] models both show excellent agreement with velocity measurements (less than 6% error). Figure 2(a) shows that the LES-2 model [8] under-predicts the centreline velocity of the inlet jet. The LNS model is here found to give best velocity predictions.

Mixing length and k–l results are not shown in the figure. However, they are substantially worse than for the k–ε model. It is hence surprising that the mixing length and to an extent

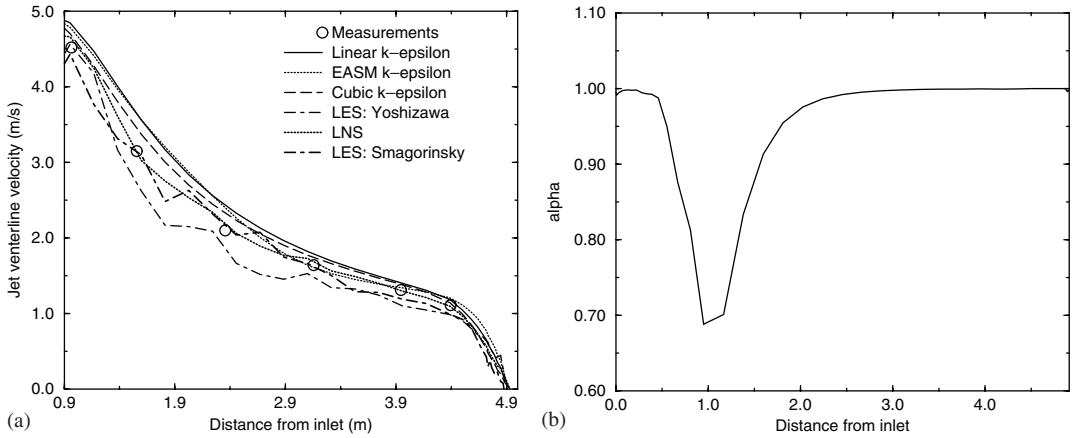

Figure 2. (a) Velocity distribution along the jet inlet centreline: predictions and measurements; and (b) turbulent viscosity damping coefficient for the LNS model.

the one equation model are so popular for room ventilation flows. Their numerical simplicity must be the over-riding attraction.

3.2. *Reynolds stresses*

Figure 3 plots the Reynolds stress τ_{xx}/ρ, τ_{yy}/ρ and τ_{zz}/ρ along the inlet jet centreline. As expected the figure shows that linear EVM are not able to predict the anisotropy of the Reynolds stress tensor. The k–ε model predicts well τ_{xx} but over-predicts τ_{yy} and τ_{zz}. The non-linear EVM (EASM and cubic), the LES-1, LES-2 and the LNS are found to predict the anisotropy of the Reynolds stress tensor. The EASM and the cubic (k–ε) predictions are found to be of similar accuracy. Excellent agreement is found between measurements and the LES-1 model. The LES-2 model accuracy is similar to that of the cubic model. It might be expected that the two LES models would give fairly similar results. The relatively large differences suggest the subgrid stress model is playing a significant role. The LNS is again found to perform well. The Reynolds stresses presented for the LNS are the sum of the contributions from the RANS and from the LES as $\tau_{ij}^{\mathrm{LNS}} = \alpha\tau_{ij}^{\mathrm{RANS}} + (1-\alpha)\tau_{ij}^{\mathrm{LES}}$ where α is the scaling coefficient applied to the turbulent viscosity of the RANS model. Figure 2(b) plots α along the inlet jet centreline. The figure highlights the hybrid nature (RANS/LES) of the LNS model. Clearly the RANS solution element is strongest. Also, the LES zone around $x = 1$ has a poor upstream boundary condition (RANS) with little resolved energy.

The differences in the Reynolds stress predictions for the different models are perhaps surprising, considering the relatively simple nature of the current room ventilation flow.

Figure 4 shows instantaneous streaklines for the cubic (k–ε), the LES-1 and LNS models. Clearly, the LNS streaklines are a compromise between the smooth RANS streaklines and the more stochastic (real-turbulence like) streaklines of the LES.

Generally speaking, in simulating room ventilation flows stagnation regions and/or slow moving re-circulation regions, where air quality is likely to be poor, are key regions of

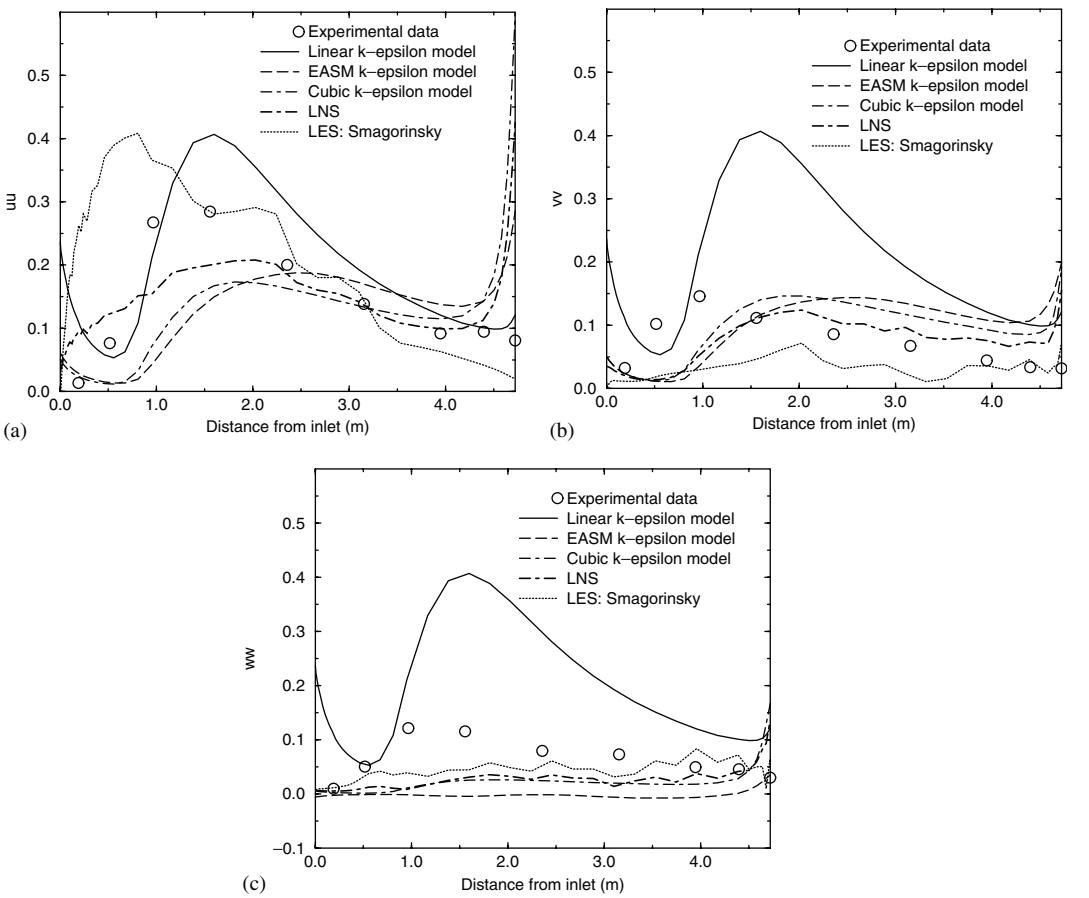

Figure 3. Centreline Reynolds stresses: (a) τ_{xx}/ρ; (b) τ_{yy}/ρ; and (c) τ_{zz}/ρ.

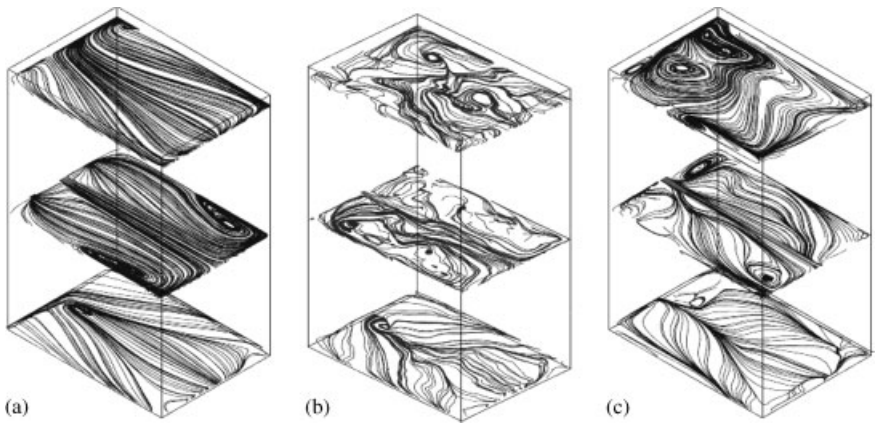

Figure 4. Streaklines: (a) Cubic k–ε; (b) LES-1; and (c) LNS model.

interest. In these areas the current RANS approaches can give qualitatively different results. This important aspect needs further exploration. By room ventilation standards the current flow is relatively benign and extreme deviations from measurements appear possible for more complex systems.

4. CONCLUSIONS

When compared to their linear equivalents, the EASM and cubic models only give minor velocity prediction improvements. The non-linear EVMs however have the advantage of capturing the anisotropy of the Reynolds stress tensor. Generally, best agreement is found between measurements and the LES-1 model. The LES-2 model under-predicts velocities at the inlet jet centreline and has similar Reynolds stress predictive accuracy to the cubic model. LNS appears as a promising model and shows here best velocity predictions (less than 5% error). LNS also predicts well Reynolds stresses and has excellent agreement with measured τ_{yy}. However, the method has the potential for LES zones to occur downstream of RANS zones. This gives rise to poor LES boundary conditions. Hence the current encouraging LNS result could be fortuitous.

REFERENCES

1. Sundell J. What we know and what we do not know about sick building syndrome. *ASHRAE Journal* 1996; **38**(6):51–62.
2. Building Amendment Regulation. Guidelines for environmental design in schools. *Architects and Building Branch*, DfEE, 2001.
3. Launder BE, Spalding DB. The numerical computation of turbulent flows. *Computer Methods in Applied Mechanics and Engineering* 1974; **3**:269–289.
4. Wolfshtein M. The velocity and temperature distribution in one-dimensional flow with turbulence augmentation and pressure gradient. *International Journal of Heat and Mass Transfer* 1969; **12**:301–318.
5. Gatski TB, Speziale CG. On explicit algebraic stress model for complex turbulent flows. *Journal of Fluid Mechanics* 1993; **254**:59–78.
6. Craft TJ, Launder BE, Suga K. Development and application of a cubic eddy viscosity model of turbulence. *International Journal of Heat and Fluid Flow* 1996; **17**:108–115.
7. Smagorinsky J. General circulation experiments with the primitive equations. I. The basic experiment. *Monthly Weather Review* 1963; **91**(3):99–165.
8. Yoshizawa A. Bridging between eddy viscosity type and second order models using a two-scale DIA. *Ninth International Symposium on Turbulent Shear Flow*, Kyoto, 1993.
9. Batten P, Goldberg U, Chakravarthy S. LNS—An approach towards embedded LES. *AIAA Paper*, *AIAA-2002-0427*, 2002.
10. He P, Kuwahara R, Mizutani K. Numerical study on air conditioned indoor airflow by dynamic large eddy simulation. *Proceeding of Indoor Air 99*, *8th International Conference on Indoor Air Quality and Climate*, Edinburgh, vol. 1. 1999; 714–719.
11. Lam CKG, Bremhorst K. A modified form of the k–ε model for predicting wall turbulence. *ASME Journal of Fluid Engineering* 1981; **103**:456–460.
12. Davidson L. Hybrid LES/RANS: a combination of a one equation SGS model and a k–ω model for predicting recirculating flows. *Proceedings of the ECCOMAS CFD Conference*, Swansea, U.K., September 2001.
13. Davidson L. A hybrid LES-RANS model based on a one-equation SGS model and a two-equation k–ω model. *The Second International Symposium on Turbulence and Shear Flow Phenomena*, Stockholm, vol. 2, 2001; 175–180.
14. Tucker PG, Davidson L. Zonal k–l based large eddy simulations. *41st AIAA Aerospace Science Meeting and Exhibit*, *AIAA-2003-0082*, Reno, Nevada, 2003.
15. Speziale CG. Turbulence modeling for time-dependent RANS and VLES: a review. *AIAA Journal* 1998; **36**(2):173–184.

16. Tucker PG. *Computation of Unsteady Internal Flows.* Kluwer Academic Publishers: Dordrecht, 2001.
17. Jouvray A. Computation and measurements of flows in rooms. *Ph.D. Thesis*, School of Engineering, University of Warwick, U.K., 2003.
18. Patankar SV, Spalding DB. A calculation procedure for heat mass and momentum transfer in three dimensional parabolic flows. *International Journal of Heat and Mass Transfer* 1972; **15**:1787–1806.

